High Order IMEX Stochastic Galerkin Schemes for Linear Transport Equation with Random Inputs and Diffusive Scalings

Zheng Chen[1*] and Lin Mu[2†]

[1*]Department of Mathematics, University of Massachusetts Dartmouth, 285 Old Westport Road, Dartmouth, 02747, MA, USA.
[2]Department of Mathematics, University of Georgia, Athens, 30602, GA, USA.

*Corresponding author(s). E-mail(s): zchen2@umassd.edu;
Contributing authors: linmu@uga.edu;
†These authors contributed equally to this work.

Abstract

In this paper, we consider the high order method for solving the linear transport equations under diffusive scaling and with random inputs. In order to tackle the randomness in the problem, the stochastic Galerkin method of the generalized polynomial chaos approach has been employed. Besides, the high order implicit-explicit scheme under the micro-macro decomposition framework and the discontinuous Galerkin method have been employed. We provide several numerical experiments to validate the accuracy and the stochastic asymptotic-preserving property.

1 Introduction

Kinetic theory connects the microscopic models with the macroscopic hydrodynamic models, and the Knudsen number is used to denote the measurement for the ratio between the particle mean free path and a typical length scale. When Knudsen number ϵ is small, the scattering rate of the particle becomes high and leads the equation to its diffusion limit. In order to overcome the expensive computational cost for stiff system in such regions, which requires fine mesh sizes and small time steps, the asymptotic-preserving (AP) schemes are designed in the discrete setting to mimic asymptotic property in the continuous setting. Thus, such a scheme becomes a consistent discretization as $\epsilon \to 0$ to mimic the asymptotic limit from the kinetic to the hydrodynamic models. AP schemes have been intensively studied in different settings and under different scalings, including [1, 15, 16, 18, 19, 21] and the review papers [12, 13, 27].

In the practical modeling, indeed, a variety of sources can bring about uncertainties to the equation , which attracts many research interests in the recent years [5, 7–9, 14, 16, 22–25]. For the stochastic linear transport equations with random inputs and under diffusive scalings, the investigation of stochastic asymptotic-preserving (sAP) schemes was proposed in [17]. Such properly designed schemes allow the mesh sizes, time steps and the number of terms in the polynomial chaos expansions independent of the Knudsen number ϵ. In this paper, we also contribute to consider the development of the robust numerical scheme, which contains the sAP properties. Here, we focus on the stochastic problem with uncertainties in collision kernels.

One popular method used in numerical simulations for kinetic problems is the Discontinuous Galerkin (DG) finite element method, which was first introduced to solve the neutron transport equation [29] employing completely discontinuous basis functions. Due to the flexibility in accepting arbitrary shapes in triangulations, the easy development in high order schemes, and the conservative properties in fundamental physics, DG methods have been widely applied to solve different partial differential equations. For the deterministic linear transport equations, the DG scheme together with the implicit–explicit (IMEX) scheme under the micro-macro decomposition was studied in [10, 11, 26, 28, 32] to achieve the AP property. Then the authors in [5] employed the similar framework with first order IMEX scheme together with the stochastic Galerkin (SG) method of the generalized polynomial chaos (gPC) approach to solve stochastic transport equations and such scheme was shown to obtain the sAP both theoretically and numerically. There are other popular numerical methods for kinetic models, such as spectral methods [3, 4, 20] and machine learning [6].

In this paper, the high order scheme with high order IMEX method is proposed to solve the stochastic linear transport equations and the sAP will be validated in our numerical experiments. The remainder of the paper is organized as follows. Section 2 discusses the general setting of the linear transport equation with random inputs and diffusive scaling, the general gPC-Galerkin framework, the micro-macro decomposition, and the diffusive limit. Section 3 introduces the fully discretized scheme, with a DG method in space and an IMEX scheme in time. The numerical tests are reported in Section 4 to validate that our proposed algorithm is high order accurate and sAP.

2 Preliminaries and Formulation

We shall consider the following discrete-velocity kinetic model in a diffusive scaling:

$$\epsilon \partial_t f + v \nabla_x f = \frac{\sigma}{\epsilon} \mathcal{L}(f), \quad \sigma(\mathbf{z}) \geq \sigma_{\min} > 0. \tag{1}$$

The function $f(t, x, v, \mathbf{z})$ is the density distribution of particles at time $t \geq 0$, position $x \in \Omega_x \subset \mathbb{R}$, velocity $v \in \{-1, 1\}$. The dimensionless Knudsen number ϵ is the ratio between particle mean free path and the characteristic length. σ is the (scaled) material cross-section. For a fixed σ, the diffusion limit corresponds to $\epsilon \to 0$, as in Section 2.3. The problem, we consider, contains uncertainties in the cross-section $\sigma(\mathbf{z})$. The uncertainty is characterized by the random vector $\mathbf{z} \in \mathbb{R}^n$, of which the components are mutually independent random variables with known probability density function $\omega(\mathbf{z})$: $I_{\mathbf{z}} \to \mathbb{R}^+$, obtained through some dimension reduction technique, e.g. Karhunen-Loève (KL) expansion. The assumptions have been described in [12]. Here $\mathcal{L}(f) = \langle f \rangle - f$ is a collision operator that describes the interactions of particles among themselves and with the medium. Moreover, $\langle f \rangle = \frac{1}{2} \left(f(x, v = -1, t) + f(x, v = 1, t) \right)$.

2.1 A gPC stochastic Galerkin framework

Following the procedure in [12, 17] or other related references, one seeks for an orthogonal polynomial expansion for the solution to problem (1), that is, for random variable $\mathbf{z} = (z_1, z_2, \cdots, z_n) \in I_{\mathbf{z}}$ (with n i.i.d. random variable),

$$f(t, x, v, \mathbf{z}) \approx f_M(t, x, v, \mathbf{z}) = \sum_{k=1}^{M} \alpha_k(t, x, v) \eta_k(\mathbf{z}) = \boldsymbol{\alpha} \cdot \boldsymbol{\eta}, \quad M = \binom{n+p}{n}. \tag{2}$$

where,

$$\boldsymbol{\alpha} = (\alpha_1, \alpha_2, \cdots, \alpha_M), \qquad \boldsymbol{\eta} = (\eta_1, \eta_2, \cdots, \eta_M).$$

Here, $\{\eta_k(\mathbf{z})\}$ are the orthonormal basis functions in $\mathbb{P}_p^n$ (the set of n-variate orthonormal polynomials of degree up to $p \geq 1$) and satisfy

$$\int_{I_{\mathbf{z}}} \eta_k(\mathbf{z}) \eta_l(\mathbf{z}) \omega(\mathbf{z}) d\mathbf{z} = \delta_{kl}, \qquad 1 \leq k, l \leq M = \dim(\mathbb{P}_p^n),$$

where, δ_{kl} is the Kronecker Delta function, and $\omega(\mathbf{z})$ is a prescribed probability density function (tensor product of the p.d.f. of z_i). The commonly used basis functions and associated weights include Hermite-Gaussian, Legendre-uniform, Laguerre-Gamma, etc. For simplicity, we consider the random dimension $n = 1$, and use $z \in I_z$ as the random variable in this paper. The method works for $\mathbf{z}$ in higher dimensions as well. For a general introduction on gPC-SG methods, we refer to [33].

2.2 Micro-macro formulation

In order to introduce the micro-macro decomposition, we introduce the orthogonal projections Π and $\mathbf{I}-\Pi$: $f = \Pi f + (\mathbf{I}-\Pi)f$, where Πf is the macroscopic part (equilibrium part of f) and $(\mathbf{I}-\Pi)f$ is the microscopic part (the fluctuation part of f) so that $\Pi f = \langle f \rangle$ and $\langle (\mathbf{I}-\Pi)f \rangle = 0$, and then to decompose the kinetic equation via the projections in terms of $\rho := \Pi f$ and $(\mathbf{I}-\Pi)f$. Here $\mathbf{I}$ is the identity operator. We shall consider the following orthogonal decomposition:

$$f = \rho + \epsilon g.$$

The previous system can be rewritten as

$$\partial_t \rho + \partial_x \langle vg \rangle = 0, \tag{3}$$

$$\partial_t g + \frac{1}{\epsilon}(\mathbf{I}-\Pi)(v\partial_x g) = -\frac{\sigma g}{\epsilon^2} - \frac{1}{\epsilon^2} v \partial_x \rho. \tag{4}$$

By applying the gPC expressions $\rho_M = \varrho \cdot \boldsymbol{\eta}$ and $g_M = G \cdot \boldsymbol{\eta}$ as in (2) to the system (3)-(4) and conduct the Galerkin projection, we obtain the following system of equations for gPC coefficient vectors $\varrho = (\rho_1, \rho_2, \cdots, \rho_M)$ and $G = (g_1, g_2, \cdots, g_M)$,

$$\partial_t \varrho + \partial_x \langle vG \rangle = 0 \tag{5}$$

$$\partial_t G + \frac{1}{\epsilon}(\mathbf{I}-\Pi)(v\partial_x G) = -\frac{1}{\epsilon^2}\mathbb{\Sigma} G - \frac{1}{\epsilon^2} v \partial_x \varrho. \tag{6}$$

Here, the matrix $\mathbb{\Sigma}$ is defined as

$$\mathbb{\Sigma} = (\sigma_{ij})_{M\times M}, \quad \text{with } \sigma_{ij} = \langle \eta_i, \sigma \eta_j \rangle_\omega \text{ for } 1 \le i,j \le M,$$

with the weighted inner product $\langle f, g \rangle_\omega := \int_{I_z} f g \omega(z) dz$. $\mathbb{\Sigma}$ is a symmetric, positive-definite matrix. Since we assume $\sigma(z) \ge \sigma_{\min} > 0$, it is easy to see that

$$\mathbb{\Sigma} \ge \sigma_{\min} \mathbb{Id},$$

where $\mathbb{Id}$ stands for the identity matrix [34].

2.3 Diffusive limit

In this subsection, we will review the equations for ρ in the limit of $\epsilon \to 0$. In the diffusion limit $\epsilon \to 0$, (3) and (4) can be approximated by the leading order of ϵ, and thus

$$v\partial_x \rho + \sigma(z) g = 0, \tag{7}$$

$$\partial_t \rho + \partial_x \langle vg \rangle = 0, \tag{8}$$

which implies

$$\partial_t \rho - \partial_x \left(\frac{1}{\sigma(z)} \partial_x \rho \right) = 0. \tag{9}$$

Similarly, equation (6) yields

$$\mathbb{\Sigma}(-G) = v \partial_x \varrho + \mathcal{O}(\epsilon)$$

and thus

$$G = -\mathbb{\Sigma}^{-1} v \partial_x \varrho + \mathcal{O}(\epsilon). \tag{10}$$

Then plugging the above equation into (5), one can obtain the limiting diffusion equation for the gPC coefficient vectors

$$\partial_t \varrho = \partial_x \left(\mathbb{\Sigma}^{-1} \partial_x \varrho \right) + \mathcal{O}(\epsilon). \tag{11}$$

When $\epsilon \to 0$, this leads to a family of limiting diffusion equations for the gPC coefficient vectors ς and $\mathcal{G}$: the limiting equation is the linear heat equation as follows

$$\partial_t \varsigma = -\partial_x Q, \qquad Q := \langle v \mathcal{G} \rangle = -\mathbb{\Sigma}^{-1} \partial_x \varsigma. \tag{12}$$

This formally shows that the gPC-SG method is sAP, in the sense of [17].

3 The Fully Discretized Scheme

In [11], a family of asymptotic preserving methods was proposed for the telegraph equation based on its micro-macro decomposition. They involve DG spatial discretization and globally stiff accurate IMEX Runge Kutta method in time. In [10], the authors extended the method to the one-group transport equation in slab geometry and established numerical stability, error estimates and a rigorous asymptotic analysis. The similar machinery in their AP deterministic studies will be employed here.

In this section, we introduce the fully discretized scheme, with DG method for the spatial discretization (Section 3.1) and high order IMEX method for the temporal discretization (Section 3.2).

3.1 Spatial Discretization: DG scheme

We first introduce some notations commonly used for DG finite element schemes [30]. Consider the spatial domain $\Omega_x = [x_L, x_R] = \bigcup_{i=1}^{N_x} I_i$, with cell $I_i = [x_{i-\frac{1}{2}}, x_{i+\frac{1}{2}}]$ of length $h_i = x_{i+\frac{1}{2}} - x_{i-\frac{1}{2}}$. Note, $x_L = x_{\frac{1}{2}}$, and $x_R = x_{N_x+\frac{1}{2}}$. The discontinuous finite element space is defined as

$$V_h^\ell = \{ u \in L^2(\Omega_x) : u|_{I_i} \in P^\ell(I_i), \forall i \in [1, \cdots, N_x] \},$$

where $P^\ell(I)$ is the polynomial space with polynomials of degree up to ℓ on cell I. Since the solution u is a piecewise polynomial, there are two values at each interface $x_{i-\frac{1}{2}}$: $u(x^+_{i-\frac{1}{2}}) = u|_{I_i}(x^+_{i-\frac{1}{2}})$ and $u(x^-_{i-\frac{1}{2}}) = u|_{I_{i-1}}(x^-_{i-\frac{1}{2}})$. We define the jump $[\![\cdot]\!]$ and average $\{\!\{\cdot\}\!\}$ of u at $x_{i-\frac{1}{2}}$ for all i to be $[\![u]\!]_{i-\frac{1}{2}} = u(x^+_{i-\frac{1}{2}}) - u(x^-_{i-\frac{1}{2}})$ and $\{\!\{u\}\!\}_{i-\frac{1}{2}} = \frac{1}{2}(u(x^+_{i-\frac{1}{2}}) + u(x^-_{i-\frac{1}{2}}))$, respectively. Moreover, on the domain boundary, we define $[\![u]\!]_{\frac{1}{2}} = u(x^+_{\frac{1}{2}})$, $[\![u]\!]_{N_x+\frac{1}{2}} = -u(x^-_{N_x+\frac{1}{2}})$ and $\{\!\{u\}\!\}_{\frac{1}{2}} = u(x^+_{\frac{1}{2}})$, $\{\!\{u\}\!\}_{N_x+\frac{1}{2}} = u(x^-_{N_x+\frac{1}{2}})$.

From (5)-(6), the DG spatial discretization of gPC-SG method is to find coefficients $\varrho_h(\cdot,t) = [\rho_{k,h}]_{k=1}^M$, $G_h(\cdot,v,t) = [g_{k,h}]_{k=1}^M$ such that $\rho_{k,h}(t,\cdot)$ and $g_{k,h}(t,\cdot,v) \in V_h^\ell$ satisfy the following equations for all test functions $\phi, \psi \in V_h^\ell$,

$$(\partial_t \rho_{k,h}, \phi) + a_h(g_{k,h}, \phi) = 0, \tag{13}$$

$$(\partial_t g_{k,h}, \psi) + \frac{1}{\epsilon} b_{h,v}(g_{k,h}, \psi) - \frac{v}{\epsilon^2} d_h(\rho_{k,h}, \psi) = -\frac{\Sigma_k}{\epsilon^2}(G_h, \psi), \tag{14}$$

where

$$a_h(g,\phi) = -\sum_{i=1}^{N_x} \int_{I_i} \langle vg \rangle \partial_x \phi dx - \sum_{i=1}^{N_x+1} \widehat{\langle vg \rangle}_{i-\frac{1}{2}} [\![\phi]\!]_{i-\frac{1}{2}}, \tag{15}$$

$$b_{h,v}(g,\psi) = \left(D_h(g,v) - \langle D_h(g,v) \rangle, \psi\right), \tag{16}$$

$$d_h(\rho,\psi) = \sum_{i=1}^{N_x} \int_{I_i} \rho \partial_x \psi dx + \sum_{i=1}^{N_x+1} \hat{\rho}_{h,i-\frac{1}{2}} [\![\psi]\!]_{i-\frac{1}{2}}, \tag{17}$$

and Σ_k is the k-th row of the matrix. Here and below, $(\cdot\ ,\cdot)$ denotes the standard inner product for the $L^2(\Omega_x;\ dx)$ space. The function $D_h(\cdot,\cdot)$ is defined based on an upwinding discretization:

$$(D_h(g,v),\psi) := -\sum_{i=1}^{N_x} \left(\int_{I_i} vg \partial_x \psi dx \right) - \sum_{i=1}^{N_x+1} \widetilde{(vg)}_{i-\frac{1}{2}} [\![\psi]\!]_{i-\frac{1}{2}}, \quad \psi \in V_h^\ell. \tag{18}$$

Besides, the upwinding flux is defined by

$$\widetilde{vg} := \begin{cases} vg^-, & \text{if } v > 0 \\ vg^+, & \text{if } v < 0; \end{cases}$$

the central flux is

$$\widehat{\langle vg \rangle} = \{\!\{\langle vg \rangle\}\!\}, \ \hat{\rho} = \{\!\{\rho\}\!\}; \tag{19}$$

and the alternating flux is

$$\widehat{\langle vg \rangle} = \langle vg \rangle^{-}, \ \hat{\rho} = \rho^{+} \text{ (left-right)} \tag{20}$$

or

$$\widehat{\langle vg \rangle} = \langle vg \rangle^{+}, \ \hat{\rho} = \rho^{-} \text{ (right-left)}. \tag{21}$$

3.2 Temporal Discretization: An IMEX Scheme

In this subsection, we further discretize the method in time with a high order IMEX. Here, we consider the uniform time step size, and thus the n-th time step $t = t^n = n\Delta t$, for all integer $n \geq 0$.

For high order temporal discretization, we use the globally stiffly accurate IMEX RK schemes. The IMEX RK schemes can be represented with pairs of Butcher tableau as follows,

$$\begin{array}{c|c} \tilde{c} & \tilde{\mathbb{A}} \\ \hline & \tilde{b}^T \end{array} \qquad \begin{array}{c|c} c & \mathbb{A} \\ \hline & b^T \end{array}$$

with $s \times s$ matrices $\tilde{\mathbb{A}} = (\tilde{a}_{ij})$ and $\mathbb{A} = (a_{ij})$, and $s \times 1$ vectors $\tilde{c}$, c, $\tilde{b}$, b.

The first order IMEX scheme is represented by

$$\begin{array}{c|cc} 0 & 0 & 0 \\ 1 & 1 & 0 \\ \hline & 1 & 0 \end{array} \qquad \begin{array}{c|cc} 0 & 0 & 0 \\ 1 & 0 & 1 \\ \hline & 0 & 1 \end{array}.$$

The second order IMEX scheme is the ARS(2,2,2) scheme with

$$\begin{array}{c|ccc} 0 & 0 & 0 & 0 \\ \gamma & \gamma & 0 & 0 \\ 1 & \delta & 1-\delta & 0 \\ \hline & \delta & 1-\delta & 0 \end{array} \qquad \begin{array}{c|ccc} 0 & 0 & 0 & 0 \\ \gamma & 0 & \gamma & 0 \\ 1 & 0 & 1-\gamma & \gamma \\ \hline & 0 & 1-\gamma & \gamma \end{array},$$

where $\gamma = 1 - \frac{1}{\sqrt{2}}$ and $\delta = 1 - \frac{1}{2\gamma}$.

The third order IMEX scheme is the ARS(4,4,3) scheme with

$$\begin{array}{c|ccccc} 0 & 0 & 0 & 0 & 0 & 0 \\ 1/2 & 1/2 & 0 & 0 & 0 & 0 \\ 2/3 & 11/18 & 1/18 & 0 & 0 & 0 \\ 1/2 & 5/6 & -5/6 & 1/2 & 0 & 0 \\ 1 & 1/4 & 7/4 & 3/4 & -7/4 & 0 \\ \hline & 1/4 & 7/4 & 3/4 & -7/4 & 0 \end{array} \qquad \begin{array}{c|ccccc} 0 & 0 & 0 & 0 & 0 & 0 \\ 1/2 & 0 & 1/2 & 0 & 0 & 0 \\ 2/3 & 0 & 1/6 & 1/2 & 0 & 0 \\ 1/2 & 0 & -1/2 & 1/2 & 1/2 & 0 \\ 1 & 0 & 3/2 & -3/2 & 1/2 & 1/2 \\ \hline & 0 & 3/2 & -3/2 & 1/2 & 1/2 \end{array}.$$

Algorithm 1 First Order DG-IMEX-gPC-SG for Transport Equations (5)-(6)

The first order DG-IMEX-gPC-SG scheme is to obtain $\rho_{k,h}^{n+1}(x)$, $g_{k,h}^{n+1}(x,v) \in V_h^\ell$, such that $\forall \phi, \psi \in V_h^\ell$, given $\rho_{k,h}^n(x)$, $g_{k,h}^n(x,v) \in V_h^\ell$ that approximate the solutions $\varrho_h(\cdot,t) = [\rho_{k,h}]_{k=1}^M$ and $G_h(\cdot,v,t) = [g_{k,h}]_{k=1}^M$ at t^n,

$$\left(\frac{\rho_{k,h}^{n+1} - \rho_{k,h}^n}{\Delta t}, \phi\right) + a_h(g_{k,h}^n, \phi) = 0, \tag{22}$$

$$\begin{aligned}\left(\frac{g_{k,h}^{n+1} - g_{k,h}^n}{\Delta t}, \psi\right) + \frac{1}{\epsilon} b_{h,v}(g_{k,h}^n, \psi) - \frac{v}{\epsilon^2} d_h(\rho_{k,h}^{n+1}, \psi) \\ = -\frac{\Sigma_k}{\epsilon^2}(G_h^{n+1}, \psi).\end{aligned} \tag{23}$$

Let us list the algorithms for the DG-IMEX-gPC-SG schemes with first order IMEX temporal discretization, followed by the schemes with high order IMEX temporal discretization, for both the transport equation (5)-(6) and diffusion limit (12).

Algorithm 2 High Order DG-IMEX-gPC-SG for Transport Equations (5)-(6)

Assume s is the total number of internal stages in the IMEX scheme, where $\ell = 1, \ldots, s$. We have the following equations true for any ϕ and $\psi \in V_h^k$:

$$(\rho_{k,h}^\ell, \phi) = (\rho_{k,h}^n, \phi) - \Delta t \sum_{j=1}^{\ell-1} \widetilde{a_{\ell,j}} a_h(g_{k,h}^j, \phi) \tag{24}$$

$$\begin{aligned}\left(g_{k,h}^\ell, \psi\right) = \left(g_{k,h}^n, \psi\right) - \Delta t \sum_{j=1}^{\ell-1} \widetilde{a_{\ell,j}} \frac{1}{\epsilon} b_{h,v}(g_{k,h}^n, \psi) \\ + \Delta t \sum_{j=1}^{\ell} \frac{a_{\ell,j}}{\epsilon^2}\left(v d_h(\rho_{k,h}^j, \psi) - \Sigma_k(G_h^j, \psi)\right).\end{aligned} \tag{25}$$

Thus, we will update

$$\rho_{k,h}^{n+1} = \rho_h^{(s)}, \text{ and } g_{k,h}^{n+1} = g_{k,h}^{(s)}.$$

Algorithm 3 First Order DG-IMEX-gPC-SG for Limiting Equations (12)

The first order DG-IMEX-gPC-SG scheme is to obtain $\varsigma_{k,h}^{n+1}(x), q_{k,h}^{n+1}(x) \in V_h^\ell$, such that $\forall \phi, \psi \in V_h^\ell$, given $\varsigma_{k,h}^n(x)$, $q_{k,h}^n(x) \in V_h^\ell$ that approximate the solutions $\varsigma_h(\cdot,t) = [\varsigma_{k,h}]_{k=1}^M$ and $Q_h(\cdot,v,t) = [q_{k,h}]_{k=1}^M$ at t^n,

$$\left(\frac{\varsigma_{k,h}^{n+1} - \varsigma_{k,h}^n}{\Delta t}, \phi\right) = -d_h(q_{k,h}^n, \phi), \tag{26}$$

$$\left(\Sigma_k Q_h^{n+1}, \psi\right) = d_h\left(\varsigma_{k,h}^{n+1}, \psi\right). \tag{27}$$

Algorithm 4 High Order DG-IMEX-gPC-SG for Limiting Equations (12)

Assume s is the total number of internal stages in the IMEX scheme, where $\ell = 1, \ldots, s$. We have the following equations true for any ϕ and $\psi \in V_h^k$:

$$(\varsigma_{k,h}^{(\ell)}, \phi) = (\varsigma_{k,h}^n, \phi) - \Delta t \sum_{j=1}^{\ell-1} \widetilde{a_{\ell,j}} d_h(q_{k,h}^{(j)}, \phi) \tag{28}$$

$$\left(\Sigma_k Q_h^{(\ell)}, \psi\right) = d_h\left(\varsigma_{k,h}^{(\ell)}, \psi\right). \tag{29}$$

Thus, we will update

$$\varsigma_{k,h}^{n+1} = \varsigma_{k,h}^{(s)}, \text{ and } q_{k,h}^{n+1} = q_{k,h}^{(s)}.$$

4 Numerical results

In this section, we shall consider the telegraph equations with $\mathcal{L}(f) = \langle f \rangle - f = -\epsilon g$ and carry out numerical tests for the accuracy check and stochastic asymptotic preserving property. In the following, we will check the errors measured by the following $L^2_{x,v,z}$ norm,

$$\|f(t,\cdot)\|_{L^2_{x,v,z}} = \left(\int_{\Omega_x \times \{-1,1\} \times (-1,1)} |f(t,x,v,z)|^2 dz dv dx\right)^{1/2}.$$

Example 4.1 Let $\Omega_x = [-\pi, \pi]$ and the exact solutions are chosen as

$$\begin{cases} \rho(t,x,z) &= \dfrac{1}{r}\exp(rt)\sin(x) \\ g(t,x,v,z) &= v\exp(rt)\cos(x) \\ q(t,x,z) &= \exp(rt)\cos(x) \end{cases} \tag{30}$$

with $r = \dfrac{-\sigma + \sqrt{-4\epsilon^2 + \sigma^2}}{2\epsilon^2}$ and $\sigma = 2 + z$ (z uniformly distributed in $(-1, 1)$), where $q = \langle vg \rangle = \frac{1}{2\epsilon}(f(v = 1) - f(v = -1))$.

In this numerical experiment, we shall employ DG element with degree $\ell = 0, 1, 2$ and IMEX scheme with order $1, 2, 3$ and gPC method with degree p. The simulation is carried out on uniform spatial meshes with totally N_x elements. The uniform time step size Δt is determined by

$$\Delta t = C_{\text{hyper}} \epsilon \Delta x + C_{\text{diff}} \Delta x^2. \tag{31}$$

4.1 Accuracy

We compare the error between the exact solution (30) and the numerical solutions of the DG-IMEX-gPC-SG scheme. We check the following two types of accuracy:

(1) DG-IMEX convergence rate: We solve the problem with $\epsilon = 10^{-2}$ using DGk-IMEX($k+1$)-gPC-SG scheme with $p = 10$, $N_x = 10, 20, 40, 80, 160$, and $k = 0, 1, 2$ up to time $T = 1$. The CFL coefficients C_{hyper} and C_{diff} in the time step size Δt (31) are chosen based on numerical tests and listed in Table 1.

k	C_{hyper}	C_{diff}
0	0.5	0.25
1	0.2	0.01
2	0.06	0.006

Table 1 CFL numbers for DGk-IMEX($k+1$)-gPC-SG methods.

We test the case with two different fluxes: central flux (19) and alternating (20) with order left-right. The errors measured in the $L^2_{x,v,z}$ norm and their orders are listed in Table 2, Table 3 and Table 4.

For the schemes with alternating flux (20), we observe $(k+1)$-th order optimal convergence for all k; for the scheme with central flux (19), we observe k-th order convergence for k odd and $(k+1)$-th order optimal convergence for k even. This one order loss of accuracy is commonly seen in local DG schemes with central flux, as stated in Section 3.1 in [31].

(2) spectral convergence with respect to the gPC order p: We solve the problem with $\epsilon = 10^{-1}, 10^{-2}, 10^{-6}$ using DG2-IMEX3-gPC-SG with alternating flux (20) and set $N_x = 400$ and $p = 1, \ldots, 7$ up to $T = 0.1$. The errors of with ratios $\text{error}_{p+1}/\text{error}_p$ are listed in Table 5. We also plot the semi-log of the errors in Figure 1. From the results, it is noted that the scheme converges in a spectral order with respect to the gPC order p.

ϵ	N_x	Central flux				Alternating flux (left-right)			
		ρ	order	q	order	ρ	order	q	order
10^{-1}	10	1.85E+0		1.18E-01		1.78E+0		2.58E-01	
	20	8.95E-01	1.04	5.91E-02	1.00	8.87E-01	1.01	1.22E-01	1.08
	40	4.44E-01	1.01	2.96E-02	1.00	4.43E-01	1.00	6.02E-02	1.02
	80	2.22E-01	1.00	1.48E-02	1.00	2.22E-01	1.00	2.99E-02	1.01
	160	1.11E-01	1.00	7.42E-03	1.00	1.11E-01	1.00	1.49E-02	1.00
10^{-2}	10	1.86E+0		1.20E-01		1.79E+0		2.53E-01	
	20	9.00E-01	1.05	5.98E-02	1.00	8.89E-01	1.01	1.21E-01	1.06
	40	4.46E-01	1.01	2.99E-02	1.00	4.45E-01	1.00	6.00E-02	1.01
	80	2.22E-01	1.00	1.49E-02	1.00	2.22E-01	1.00	2.99E-02	1.00
	160	1.11E-01	1.00	7.47E-03	1.00	1.11E-01	1.00	1.49E-02	1.00
10^{-6}	10	1.86E+0		1.20E-01		1.79E+0		2.52E-01	
	20	9.00E-01	1.05	5.99E-02	1.00	8.89E-01	1.01	1.21E-01	1.06
	40	4.46E-01	1.01	2.99E-02	1.00	4.45E-01	1.00	6.00E-02	1.01
	80	2.22E-01	1.00	1.49E-02	1.00	2.22E-01	1.00	2.99E-02	1.00
	160	1.11E-01	1.00	7.47E-03	1.00	1.11E-01	1.00	1.49E-02	1.00

Table 2 DG0-IMEX1 convergence rate with gPC order $p = 10$ at $T = 1$, with $C_{\text{hyper}} = 0.5, C_{\text{diff}} = 0.25$.

ϵ	N_x	Central flux				Alternating flux (left-right)			
		ρ	order	q	order	ρ	order	q	order
10^{-1}	10	4.29E-01		2.15E-01		2.36E-01		1.02E-01	
	20	2.12E-01	1.02	1.05E-01	1.03	5.88E-02	2.01	2.51E-02	2.02
	40	1.06E-01	1.00	5.24E-02	1.01	1.47E-02	2.00	6.26E-03	2.00
	80	5.29E-02	1.00	2.62E-02	1.00	3.67E-03	2.00	1.56E-03	2.00
	160	2.64E-02	1.00	1.31E-02	1.00	9.18E-04	2.00	3.91E-04	2.00
10^{-2}	10	4.30E-01		2.15E-01		2.37E-01		1.02E-01	
	20	2.13E-01	1.02	1.06E-01	1.03	5.90E-02	2.01	2.52E-02	2.02
	40	1.06E-01	1.00	5.25E-02	1.01	1.47E-02	2.00	6.27E-03	2.00
	80	5.30E-02	1.00	2.62E-02	1.00	3.68E-03	2.00	1.57E-03	2.00
	160	2.65E-02	1.00	1.31E-02	1.00	9.20E-04	2.00	3.92E-04	2.00
10^{-6}	10	4.30E-01		2.16E-01		2.37E-01		1.02E-01	
	20	2.13E-01	1.02	1.06E-01	1.03	5.90E-02	2.01	2.52E-02	2.02
	40	1.06E-01	1.00	5.25E-02	1.01	1.47E-02	2.00	6.27E-03	2.00
	80	5.30E-02	1.00	2.62E-02	1.00	3.68E-03	2.00	1.57E-03	2.00
	160	2.65E-02	1.00	1.31E-02	1.00	9.20E-04	2.00	3.92E-04	2.00

Table 3 DG1-IMEX2 convergence rate with gPC order $p = 10$ at $T = 1$, with $C_{\text{hyper}} = 0.2, C_{\text{diff}} = 0.01$.

4.2 Stochastic Asymptotic Preserving (sAP) Property

Next, we check the stochastic asymptotic preserving property of the proposed DG-IMEX-gPC-SG scheme with high order IMEX temporal discretization. We will show that for fixed $\Delta t, h, M$, as the Knudsen number $\epsilon \to 0$, the limiting scheme of DG-IMEX-gPC-SG is a consistent DG-IMEX discretization for the Galerkin system of the limiting diffusion equation.

ϵ	N_x	Central flux				Alternating flux (left-right)			
		ρ	order	q	order	ρ	order	q	order
10^{-1}	10	8.03E-03		3.42E-03		1.18E-02		5.05E-03	
	20	9.66E-04	3.06	4.12E-04	3.06	1.48E-03	3.00	6.30E-04	3.00
	40	1.20E-04	3.01	5.10E-05	3.01	1.85E-04	3.00	7.88E-05	3.00
	80	1.49E-05	3.00	6.36E-06	3.00	2.31E-05	3.00	9.85E-06	3.00
	160	1.87E-06	3.00	8.00E-07	2.99	2.89E-06	3.00	1.23E-06	3.00
10^{-2}	10	8.05E-03		3.43E-03		1.19E-02		5.05E-03	
	20	9.69E-04	3.06	4.12E-04	3.06	1.48E-03	3.00	6.31E-04	3.00
	40	1.20E-04	3.01	5.11E-05	3.01	1.85E-04	3.00	7.89E-05	3.00
	80	1.50E-05	3.00	6.37E-06	3.00	2.32E-05	3.00	9.86E-06	3.00
	160	1.87E-06	3.00	8.01E-07	2.99	2.90E-06	3.00	1.24E-06	3.00
10^{-6}	10	8.05E-03		3.43E-03		1.19E-02		5.05E-03	
	20	9.69E-04	3.06	4.12E-04	3.06	1.48E-03	3.00	6.31E-04	3.00
	40	1.20E-04	3.01	5.11E-05	3.01	1.85E-04	3.00	7.89E-05	3.00
	80	1.50E-05	3.00	6.37E-06	3.00	2.32E-05	3.00	9.86E-06	3.00
	160	1.87E-06	3.00	8.01E-07	2.99	2.90E-06	3.00	1.24E-06	3.00

Table 4 DG2-IMEX3 convergence rate with gPC order $p = 10$ at $T = 1$, with $C_{\text{hyper}} = 0.06, C_{\text{diff}} = 0.006$.

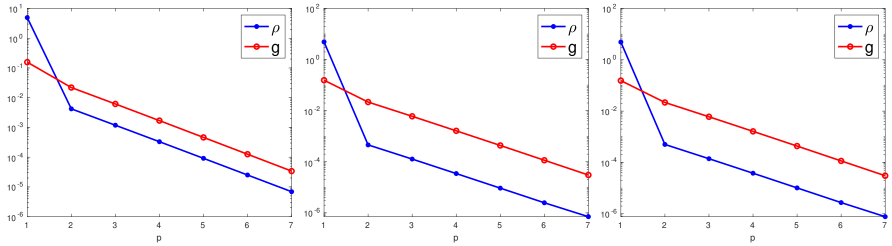

(a) $\epsilon = 10^{-1}$ (b) $\epsilon = 10^{-2}$ (c) $\epsilon = 10^{-6}$

Fig. 1 The total $L^2_{x,v,z}$ errors in ρ and g w.r.t. the gPC orders $p = 1, \ldots, 7$ for DG2-IMEX3-gPC-SG with alternating flux (20) at $T = 0.1$, where $\epsilon = 10^{-1}, 10^{-2}$ and 10^{-6} and $N_x = 400$.

In this test, we apply DG2-IMEX3-gPC12-SG on a spatial mesh with fixed cell number $N_x = 160$, and set the time stepping size $\Delta t = 0.006\Delta x^2$ and final time $T = 0.0001$. We compute and compare the numerical solutions of the limiting scheme (28)-(29) on the diffusion limit equation (9) and the proposed scheme (24)-(25) on the micro-macro system (3)-(4). In Figure 2, the expectations and variations of the densities are plotted: the red curves are for the diffusion limit, and the blue ones are the solutions to the proposed scheme with parameter $\epsilon = 1/2, 1/4$ and $1/8$. Figure 2 shows that the solutions to the micro–macro system converge to that of the limit diffusion system as $\epsilon \to 0$, which implies the sAP property.

Furthermore, the convergence test has been conducted to show the rate of errors with respect to ϵ of micro–macro system to diffusion limit system, for fixed Δx and Δt. The differences of the expectations and variations between

	$\epsilon = 10^{-1}$				$\epsilon = 10^{-2}$				$\epsilon = 10^{-6}$			
p	ρ	Ratio	g	Ratio	ρ	Ratio	g	Ratio	ρ	Ratio	g	Ratio
1	4.94E+00		1.57E-01		4.92E+00		1.56E-01		4.92E+00		1.55E-01	
2	4.23E-03	0.00	2.20E-02	0.14	4.59E-04	9.32E-05	2.18E-02	0.14	5.04E-04	1.02E-04	2.18E-02	0.14
3	1.19E-03	0.28	6.17E-03	0.28	1.28E-04	0.28	6.04E-03	0.28	1.40E-04	0.28	6.04E-03	0.28
4	3.32E-04	0.28	1.70E-03	0.28	3.47E-05	0.27	1.63E-03	0.27	3.81E-05	0.27	1.63E-03	0.27
5	9.17E-05	0.28	4.63E-04	0.27	9.31E-06	0.27	4.36E-04	0.27	1.02E-05	0.27	4.36E-04	0.27
6	2.52E-05	0.28	1.26E-04	0.27	2.49E-06	0.27	1.15E-04	0.26	2.73E-06	0.27	1.15E-04	0.26
7	6.93E-06	0.27	3.41E-05	0.27	7.11E-07	0.29	3.04E-05	0.26	7.71E-07	0.28	3.04E-05	0.26

Table 5 The total $L^2_{x,v,z}$ errors in ρ and g w.r.t. the gPC orders $p = 1, \dots, 7$ for DG2-IMEX3-gPC-SG with alternating flux (20), where $N_x = 400$, $T = 0.1$ and $\epsilon = 10^{-1}, 10^{-2}, 10^{-6}$.

the numerical solutions of the limit equation and the micro–macro system are measured in $L^2_x[-\pi, \pi]$ norm and presented, together with the ϵ-orders, in Table 6. One can observe that the convergence rate with respect to ϵ is of order $\mathcal{O}(\epsilon^2)$ before saturating to the level of accuracy, due to the dominancy by the spacial and temporal errors. This numerical observation confirms that the proposed scheme accurately preserves the diffusion limit asymptotics up to $\mathcal{O}(\epsilon^2)$. Similar AP property has been numerically observed for a numerical method for the Boltzmann equation based on the micro-macro decomposition technique preserving the compressible Navier–Stokes asymptotics [2].

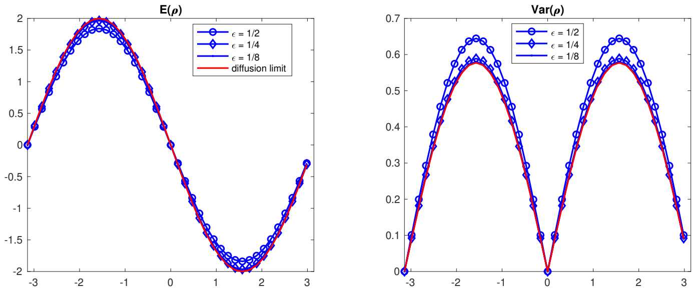

Fig. 2 The expectation and variance in numerical solution ρ to the limit equaion and kinetic system with different values of ϵ at $T = 0.0001$. (DG2-IMEX3-gPC-SG with central flux and gPC orders $p = 12$, where $N_x = 160$.)

ϵ	diff. in E(ρ)	order	diff. in Var(ρ)	order
1/2	2.83E-01		1.19E-01	
1/4	6.25E-02	2.18	2.04E-02	2.55
1/8	1.53E-02	2.03	4.82E-03	2.08
1/16	3.78E-03	2.02	1.19E-03	2.02
1/32	9.20E-04	2.04	2.96E-04	2.00
1/64	2.06E-04	2.16	7.39E-05	2.00
1/128	2.79E-05	2.89	1.85E-05	2.00
1/256	1.67E-05	0.74	4.62E-06	2.00

Table 6 The difference between expectation and variance in numerical solution ρ to the limit equation and kinetic system with different values of ϵ at $T = 0.0001$, measured in $L^2_x[-\pi, \pi]$. DG2-IMEX3-gPC-SG with central flux and gPC orders $p = 12$, where $N_x = 160$.

5 Conclusions and discussion

In this paper, we have applied the high order IMEX scheme together with gPC to solve the stochastic linear transport equations. The sAP has been observed in the scheme, and thus validates our algorithm. The developed sAP scheme is applicable to the other discrete-velocity kinetic equations under a diffusive scaling. The sAP property for more complex system, such as the ones with multi-dimensional random variables, and the models with a spatially dependent scattering kernel, will be investigated in the future work.

Ethical Statement

i. Compliance with Ethical Standards
This article does not contain any studies involving animals performed by any of the authors. This article does not contain any studies involving human participants performed by any of the authors.

ii. Funding
Mu is partial supported by the Simons Foundation: Collaboration Grants. Chen is partial supported by the AFOSR grant FA9550-18-1-0383.

iii. Conflict of Interest
On behalf of all authors, the corresponding author states that there is no conflict of interest.

References

[1] J. A. Carrillo, T. Goudon, P. Lafitte, and F. Vecil, Numerical schemes of diffusion asymptotics and moment closures for kinetic equations, Journal of Scientific Computing, 36 (2008), pp. 113–149.

[2] M. Bennoune, M. Lemou, L. Mieussens, Uniformly stable numerical schemes for the Boltzmann equation preserving the compressible Navier–Stokes asymptotics, Journal of Computational Physics 227 8 (2008) 3781–3803.

[3] Y. Chen, Z. Chen, Z., Y. Cheng, A. Gillman, F. Li, Study of Discrete Scattering Operators for Some Linear Kinetic Models. Topics In Numerical Partial Differential Equations And Scientific Computing. pp. 99-136 (2016)

[4] Z. Chen, C.D. Hauck, Multiscale convergence properties for spectral approximations of a model kinetic equation. Mathematics Of Computation. 88, 2257-2293 (2019)

[5] Z. Chen, L. Liu, L. Mu, DG-IMEX stochastic Galerkin schemes for linear transport equation with random inputs and diffusive scalings, Journal of Scientific Computing 73 (2017) 566–592.

[6] Z. Chen, L. Mu, Solving the linear transport equation by a deep neural network approach. Discrete And Continuous Dynamical Systems - S. 15(4) pp. 669-686 (2022)

[7] E. Daus, S. Jin, L. Liu, On the multi-species Boltzmann equation with uncertainty and its stochastic Galerkin approximation. ESAIM: Mathematical Modelling and Numerical Analysis. 55, 1323-1345 (2021)

[8] J. Escalante,C. Heitzinger, Stochastic Galerkin methods for the Boltzmann-Poisson system. Journal of Computational Physics. 466 pp. 111400 (2022)

[9] J. Hu, S. Jin, Uncertainty quantification for kinetic equations. Uncertainty Quantification for Hyperbolic and Kinetic Equations. pp. 193-229 (2017)

[10] J. Jang, F. Li, J. Qiu, T. Xiong, Analysis of asymptotic preserving DG-IMEX schemes for linear kinetic transport equations in a diffusive scaling, SIAM J. Numer. Anal. 52 (2014) 2048–2072.

[11] J. Jang, F. Li, J. Qiu, T. Xiong, High order asymptotic preserving DG-IMEX schemes for discrete-velocity kinetic equations in a diffusive scaling, J. Comput. Phys. 281 (2015) 199–224.

[12] S. Jin, Asymptotic-preserving schemes for multiscale physical problems, Acta Numerica 31 (2022) 415–489.

[13] S. Jin. Asymptotic preserving (AP) schemes for multiscale kinetic and hyperbolic equations: a review. Lecture notes for summer school on methods and models of kinetic theory (M&MKT), Porto Ercole (Grosseto, Italy). 2010 Jun:177-216.

[14] S. Jin, Mathematical analysis and numerical methods for multiscale kinetic equations with uncertainties. Proceedings of the International Congress of Mathematicians: Rio De Janeiro 2018. pp. 3611-3639 (2018)

[15] S. Jin, J. Liu and Z. Ma, Uniform spectral convergence of the stochastic Galerkin method for the linear transport equations with random inputs in diffusive regime and a micro-macro decomposition based asymptotic preserving method,Research in the Mathematical Sciences. 4 (2017), 15.

[16] S. Jin, H. Lu, L. Pareschi, Efficient stochastic asymptotic-preserving implicit-explicit methods for transport equations with diffusive scalings and random inputs. SIAM Journal on Scientific Computing. 40, A671-A696 (2018)

[17] S. Jin, D. Xiu, X. Zhu, Asymptotic-preserving methods for hyperbolic and transport equations with random inputs and diffusive scalings. Journal of Computational Physics. 289, 35–52 (2015)

[18] A. Klar, An asymptotic-induced scheme for nonstationary transport equations in the diffusive limit, SIAM Journal on Numerical Analysis, 35 (1998), pp. 1073–1094.

[19] P. Lafitte and G. Samaey, Asymptotic-preserving projective integration schemes for kinetic equations in the diffusion limit, SIAM Journal on Scientific Computing, 34 (2012), pp. 579–602.

[20] M. Laiu, Z. Chen, C.D. Hauck, A fast implicit solver for semiconductor models in one space dimension. Journal Of Computational Physics. 417 pp. 109567 (2020)

[21] M. Lemou and L. Mieussens, A new asymptotic preserving scheme based on micro-macro formulation for linear kinetic equations in the diffusion limit, SIAM Journal on Scientific Computing, 31 (2010), pp. 334– 368.

[22] L. Liu, A Bi-Fidelity DG-IMEX Method for the Linear Transport Equation with Random Parameters. ECCOMAS Congress 2020. (2021)

[23] L. Liu, A stochastic asymptotic-preserving scheme for the bipolar semiconductor Boltzmann-Poisson system with random inputs and diffusive scalings. Journal of Computational Physics. 376 pp. 634-659 (2019)

[24] L. Liu, Uniform spectral convergence of the stochastic Galerkin method for the linear semiconductor Boltzmann equation with random inputs and diffusive scalings. Kinetic and Related Models. 11(5) pp. 1139-1156 (2018)

[25] L. Liu, S. Jin, Hypocoercivity based sensitivity analysis and spectral convergence of the stochastic Galerkin approximation to collisional kinetic equations with multiple scales and random inputs, Multiscale Modeling & Simulation 16 (2018) 1085-1114.

[26] R.B. Lowrie and J.E. Morel. Methods for hyperbolic systems with stiff relaxation. International Journal for Numerical Methods in Fluids. 40(2002):413-23.

[27] L. Pareschi, G. Russo. Efficient asymptotic preserving deterministic methods for the Boltzmann equation. Lecture Series held at the von Karman Institute,Rhode St. Gense, Belgium, AVT-194 RTO AVT/VKI, (2011)

[28] Z. Peng, Y. Cheng, J.-M. Qiu, F. Li, Stability-enhanced AP IMEX-LDG schemes for linear kinetic transport equations under a diffusive scaling (2018).

[29] W.H. Reed and T.R. Hill. Triangular mesh methods for the neutron transport equation. Los Alamos Scientific Lab., N. Mex.(USA); 1973.

[30] C.W. Shu, Discontinuous Galerkin methods: general approach and stability, numerical solutions of partial differential equations, Advanced courses in Mathematics CRM Barcelona, Birkhäuser, Basel (2009) 149–201.

[31] C.W. Shu, Discontinuous Galerkin method for time-dependent problems: survey and recent developments, In: Feng, X., Karakashian, O., Xing, Y. (eds) Recent Developments in Discontinuous Galerkin Finite Element Methods for Partial Differential Equations. The IMA Volumes in Mathematics and its Applications, vol 157. Springer, Cham. 2014.

[32] T. Xiong, J. Jang, F. Li, J. Qiu, High order asymptotic preserving nodal discontinuous Galerkin IMEX schemes for the BGK equation, Journal of Computational Physics 284 (2015) 70–94.

[33] D. Xiu, Numerical methods for stochastic computations: a spectral method approach, In Numerical Methods for Stochastic Computations. Princeton university press. 2010.

[34] D. Xiu, J. Shen, Efficient stochastic Galerkin methods for random diffusion equations, Journal of Computational Physics 228 (2009) 266–281.